Bacterial metabolism of tryptophan causes toxicity in *Caenorhabditis elegans*

Shivani Gahlot[1], Subodh[1], and Jogender Singh[1,*]

[1]Department of Biological Sciences, Indian Institute of Science Education and Research, Mohali, Punjab, 140306, India

[*]For correspondence: jogender@iisermohali.ac.in

Keywords: indole; microbiota; sugars; tryptophan; tryptophanase

Abstract

Tryptophan is an essential amino acid required not only for protein biosynthesis but also for the production of several physiologically important metabolites, including serotonin, kynurenine, and nicotinamide. Although dietary tryptophan is associated with various health benefits, excessive intake can result in adverse physiological effects. The specific tryptophan-derived metabolites responsible for such toxicity, however, remain incompletely characterized. Here, we investigate the mechanisms underlying tryptophan-induced toxicity in *Caenorhabditis elegans*. We observe that tryptophan concentrations of 1 mM or higher are highly toxic to *C. elegans*, blocking egg hatching. Notably, supplementation with various sugars alleviates this toxicity. Genetic analyses reveal that host tryptophan metabolism is dispensable for the observed effects. Instead, bacterial metabolism, particularly the conversion of tryptophan to indole, is essential for mediating toxicity. Bacterial strains deficient in indole production abolished tryptophan-induced toxicity, and all sugars that conferred protection also suppressed bacterial indole synthesis. These findings demonstrate that tryptophan toxicity in *C. elegans* is primarily mediated by microbial metabolism and underscore the pivotal role of host-microbiota interactions in shaping the physiological consequences of dietary amino acid intake.

Introduction

Tryptophan is an essential amino acid that is obtained exclusively through the diet. Beyond its fundamental role in protein biosynthesis, tryptophan regulates diverse physiological processes. It serves as a precursor for several bioactive molecules, including nicotinamide, serotonin, tryptamine, melatonin, and kynurenine, which participate in key metabolic and signaling pathways (Gao *et al*, 2020; Xue *et al*, 2023). As the sole precursor of the neurotransmitter serotonin, tryptophan is vital for maintaining optimal neurological and physiological function (Fernstrom, 1983). Systemic or oral administration of tryptophan enhances serotonin synthesis (Haleem, 2023), supporting its use as a dietary supplement to improve sleep quality and mood, and to manage psychiatric conditions such as depression and anxiety (Lindseth *et al*, 2015).

Emerging evidence suggests that dietary tryptophan and its metabolites may have therapeutic potential in various pathological conditions, including microbial infections, multiple sclerosis, inflammatory bowel disease, chronic kidney disease, and cardiovascular disease (Agus *et al*, 2018; Haleem, 2023; Xue *et al*, 2023). In rodent models, tryptophan supplementation has been shown to lower blood glucose levels in type 2 diabetic rats (Inubushi *et al*, 2012). In *Caenorhabditis elegans*, elevated tryptophan levels, either through direct supplementation or inhibition of its catabolism, have been linked to increased lifespan (van der Goot *et al*, 2012; Edwards *et al*, 2015; Dang *et al*, 2023). Additional studies suggest that high dietary intake of tryptophan may protect against intestinal inflammation (Zhang *et al*, 2021). Tryptophan fortification of foods has also been associated with improved sleep in infants with sleep disorders, weight gain in malnourished children, and enhanced mood and sleep quality in elderly individuals (Cubero *et al*, 2009; Friedman, 2018).

Despite these benefits, excessive tryptophan intake has also been associated with adverse outcomes (Hu *et al*, 2023; Izadi *et al*, 2024). In rodents, dietary restriction of tryptophan has been shown to extend lifespan and delay the onset of age-associated pathologies, including tumor development (Ooka *et al*, 1988; Segall & Timiras, 1976). Interestingly, the non-steroidal anti-inflammatory drug ibuprofen extends lifespan in yeast, worms, and flies by inhibiting tryptophan uptake (He *et al*, 2014). Although a minor fraction of dietary tryptophan is utilized for serotonin and tryptamine synthesis, over 95% is catabolized via the kynurenine pathway (Le Floc'h *et al*, 2011; Xue *et al*, 2023). Elevated levels of kynurenine pathway metabolites have been implicated in autoimmune diseases, neurodegenerative disorders, and various cancers (Schwarcz & Stone, 2017). Additionally,

gut microbiota metabolize tryptophan into indole and its derivatives, which can be further converted in the liver into indoxyl sulfate, a uremic toxin associated with oxidative stress and tissue injury (Agus *et al*, 2018; Graboski & Redinbo, 2020). Given that tryptophan has both beneficial and detrimental effects, it is critical to elucidate the mechanisms underlying its toxicity and to better understand the regulation of its metabolism in host-microbe interactions.

In this study, we investigated the mechanisms underlying tryptophan toxicity in *C. elegans*. We found that tryptophan was highly toxic at concentrations of 1 mM or greater, leading to a complete inhibition of egg hatching. Interestingly, supplementation with various sugars alleviated this toxicity. Genetic analyses revealed that host tryptophan metabolic pathways were not required for the manifestation of toxic effects. Instead, microbial metabolism of tryptophan played a central role in mediating toxicity. Specifically, the bacterial conversion of tryptophan into indole was responsible for the deleterious effects, and bacterial diets lacking the ability to produce indole abolished tryptophan toxicity. Notably, all sugars that alleviated tryptophan toxicity also inhibited bacterial indole production. Our findings reveal that tryptophan toxicity in *C. elegans* is driven by microbial metabolism and demonstrate the critical role of the host-microbiota axis in shaping the physiological outcomes of dietary amino acid intake.

Results

Tryptophan is highly toxic to *C. elegans* and inhibits egg hatching

While rearing *C. elegans* on *Escherichia coli* OP50-seeded nematode growth medium (NGM) plates supplemented with various amino acids, we observed that tryptophan was highly toxic. At concentrations of 2 mM or higher, tryptophan completely inhibited egg hatching (Figure 1A, B). This observation is consistent with a recent study (Ke *et al*, 2020), which reported that tryptophan exhibited the highest toxicity among the 20 standard amino acids, significantly impairing *C. elegans* development. In our assays, toxic effects were evident at 1 mM tryptophan, where more than half of the eggs failed to hatch, and at 2 mM, no hatching occurred (Figure 1A, B).

To investigate the mechanisms underlying tryptophan toxicity, we performed RNA sequencing to profile transcriptional changes following a 6-hour exposure of adult wild-type

N2 worms to 2 mM tryptophan. Transcriptome analysis revealed 1,625 differentially expressed genes, including 963 upregulated and 662 downregulated transcripts (Figure 1C, Table S1). Gene Ontology (GO) analysis of the upregulated genes revealed significant enrichment in biological processes related to innate immune and xenobiotic responses (Figure 1D). In terms of molecular function, the upregulated genes were enriched for monooxygenase and oxidoreductase activities, including several members of the cytochrome P450 and UDP-glucuronosyltransferase (UGT) families (Figure S1A). These findings suggested activation of xenobiotic detoxification pathways in response to tryptophan exposure. Conversely, GO analysis of downregulated genes indicated enrichment in terms associated with cuticle structure and transmembrane transport (Figure S1B, C).

Sugars rescue tryptophan toxicity

Interestingly, GO analysis also revealed that genes involved in monosaccharide and hexose transport were upregulated upon tryptophan exposure (Figures 1D and S1A), suggesting a possible interaction between sugar metabolism and tryptophan toxicity. To explore this, we supplemented NGM plates containing 10 mM tryptophan with various monosaccharides at a concentration of 50 mM. Notably, while these monosaccharides alone did not affect *C. elegans* development in the absence of tryptophan (Figure S2A), they fully rescued the toxic effects of tryptophan (Figure 2A, B). Egg hatching was restored on plates containing 10 mM tryptophan supplemented with D-glucose, D-fructose, D-mannose, D-galactose, or L-rhamnose, whereas no hatching occurred on plates with 10 mM tryptophan alone.

We further tested whether disaccharides could similarly suppress tryptophan toxicity. To this end, we supplemented tryptophan-containing plates with lactose, sucrose, or maltose. Interestingly, only lactose supplementation rescued tryptophan-induced toxicity (Figure 2A, B). Neither sucrose nor maltose restored egg hatching in the presence of tryptophan. Importantly, all three disaccharides supported normal development in the absence of tryptophan (Figure S2A), indicating that the inability of sucrose and maltose to rescue was not due to inherent developmental toxicity.

To determine whether lower concentrations of sugar could also rescue tryptophan toxicity, we supplemented 10 mM tryptophan plates with varying concentrations of glucose and assessed egg hatching. No rescue was observed at 2 mM glucose, whereas glucose

concentrations of 5 mM and above fully restored egg hatching (Figures 2C and S2B), demonstrating a dose-dependent protective effect.

Next, we examined whether glucose supplementation could reverse the transcriptional changes induced by tryptophan exposure. RNA sequencing analysis of adult N2 worms exposed to 2 mM tryptophan plus 50 mM glucose for 6 hours showed a marked reduction in transcriptomic perturbation. (Table S2). Only 244 genes were upregulated under the tryptophan-plus-glucose condition, compared to 963 genes upregulated in response to tryptophan alone (Figure 2D). Notably, 806 of the genes upregulated in the tryptophan-only condition were no longer upregulated when glucose was present (Table S3). Moreover, most of the 157 genes upregulated in both conditions exhibited higher expression levels under tryptophan-only exposure than with tryptophan plus glucose (Figure 2E). A similar trend was observed among downregulated genes, with a sharp reduction in the number of genes downregulated under the tryptophan-plus-glucose condition compared to tryptophan alone (Figure S3, Table S4). Collectively, these findings demonstrated that glucose supplementation effectively rescues tryptophan-induced toxicity at both the developmental and transcriptional levels.

Blocking tryptophan catabolism in *C. elegans* does not alleviate tryptophan toxicity

To understand how sugars mitigate tryptophan-induced toxicity, we first investigated whether excess tryptophan is metabolized into a toxic downstream product, and whether sugars act by suppressing the production or activity of this metabolite. In *C. elegans*, as in other eukaryotes, tryptophan is catabolized via three primary pathways: the kynurenine, serotonin, and indole branches (Figure 3A). The kynurenine pathway accounts for over 95% of dietary tryptophan metabolism, and elevated kynurenine/tryptophan ratios have been associated with a variety of pathological conditions (Xue *et al*, 2023). We therefore hypothesized that a toxic metabolite produced through the kynurenine pathway may underlie the observed developmental toxicity.

To test this hypothesis, we examined *tdo-2* mutants, which lack tryptophan-2,3-dioxygenase, the rate-limiting enzyme that initiates kynurenine synthesis. If toxicity were mediated by kynurenine-derived metabolites, *tdo-2* loss-of-function mutants would be expected to exhibit resistance to tryptophan toxicity. However, *tdo-2(ve552)*

mutants failed to hatch on 2 mM tryptophan, displaying sensitivity comparable to that of wild-type N2 animals (Figure 3B, C).

We next asked whether the serotonin or indole branches of tryptophan metabolism contribute to toxicity. Mutants defective in serotonin synthesis (*tph-1(mg280)*) or indole production (*amx-2(ok1235)*) were exposed to 2 mM tryptophan. Eggs from both mutant strains failed to hatch, showing no resistance relative to N2 (Figure 3B, C). Taken together, these results indicated that blocking any single host-mediated tryptophan catabolic pathway does not rescue tryptophan toxicity in *C. elegans*.

Bacterial metabolism of tryptophan is essential for its toxicity in *C. elegans*

Since host-mediated tryptophan catabolism did not appear to underlie tryptophan toxicity, we investigated whether bacterial metabolism of tryptophan contributes to the toxic effects observed in *C. elegans*. To test this, we transferred *C. elegans* eggs to unseeded NGM plates containing 10 mM tryptophan and monitored their hatching. It is well established that *C. elegans* eggs can hatch in the absence of food and arrest at the L1 larval stage. While eggs fail to hatch on *E. coli* OP50-seeded plates containing 10 mM tryptophan, the use of unseeded plates enables assessment of tryptophan toxicity in the absence of bacterial metabolism. Strikingly, all eggs transferred to unseeded plates containing 10 mM tryptophan hatched successfully (Figure S4A, B). This observation strongly suggested that active bacterial metabolism is required for tryptophan-induced toxicity.

To validate this finding, we monitored the hatching of *C. elegans* eggs on 10 mM tryptophan plates seeded with kanamycin-killed *E. coli* OP50. Notably, in the presence of dead bacteria, tryptophan did not impair egg hatching or subsequent development; all worms developed to become fertile adults (Figure 4A, B). Together, these results indicated that active bacterial metabolism of tryptophan generates a toxic product that mediates the observed effects in *C. elegans*.

In *E. coli*, tryptophan is primarily metabolized via the indole pathway (Lee & Lee, 2010). Specifically, the bacterial enzyme tryptophanase (TnaA) catalyzes the conversion of tryptophan into indole, pyruvate, and ammonia (Smith, 1897). We therefore hypothesized that indole production by *E. coli* mediates the observed toxicity. To test this, we utilized an *E. coli* Δ*tnaA* mutant, which lacks tryptophanase, and assessed *C. elegans* egg hatching on 10 mM tryptophan plates seeded with this mutant strain. Strikingly, all eggs hatched and developed

normally on 10 mM tryptophan plates seeded with *E. coli* Δ*tnaA* (Figure 4C, D), confirming that the toxic effect of tryptophan required its conversion to indole by bacterial TnaA.

To further substantiate this conclusion, we examined whether tryptophan was toxic when metabolized by a bacterium that does not produce indole. *Pseudomonas aeruginosa* catabolizes tryptophan via the oxidative kynurenine pathway, generating anthranilate rather than indole (Bortolotti *et al*, 2016). When *C. elegans* eggs were cultured on 10 mM tryptophan plates seeded with *P. aeruginosa*, all eggs hatched, and no toxicity was observed (Figure 4E, F). Together, these data demonstrated that the production of indole by bacterial tryptophanase is responsible for the toxic effects of tryptophan in *C. elegans*.

Indole causes toxicity in *C. elegans*

To directly assess whether indole causes toxicity in *C. elegans*, we supplemented NGM plates with indole and examined its effect on egg hatching. Similar to the effects observed with tryptophan, indole supplementation on *E. coli* OP50-seeded plates inhibited egg hatching, with toxic effects evident at concentrations of 1 mM and above (Figure 5A, B). Since *P. aeruginosa* rescued the toxic effects of tryptophan, we next investigated whether it could similarly attenuate indole-induced toxicity. However, indole remained toxic on *P. aeruginosa*-seeded plates, and no eggs hatched at concentrations of 2 mM or higher (Figure 5A, B). At 1 mM indole, a significantly greater number of eggs hatched on *P. aeruginosa*-seeded plates compared to those seeded with *E. coli*. This difference is likely attributable to the endogenous production of indole by *E. coli*, which *P. aeruginosa* does not produce, resulting in a higher effective concentration of indole in the *E. coli*-seeded condition.

To determine whether bacterial presence is required for indole toxicity, we examined egg hatching on both unseeded and *E. coli*-seeded indole plates. Notably, egg hatching was similarly inhibited on unseeded plates containing 2 mM indole (Figures 5C and S5A), indicating that indole exerts its toxic effects independently of live bacteria. Similarly, indole inhibited egg hatching on plates seeded with kanamycin-killed *E. coli* (Figure 5D, E), further confirming that bacterial viability is not required for indole-induced toxicity.

We also tested whether the *E. coli* Δ*tnaA* mutant, which lacks tryptophanase and cannot convert tryptophan to indole, could alter indole toxicity. Importantly, the Δ*tnaA*

mutant did not mitigate indole toxicity, as eggs failed to hatch on 2 mM indole plates seeded with this strain (Figure 5F, G). Collectively, these findings demonstrate that indole itself is inherently toxic to *C. elegans*, and this toxicity is independent of bacterial metabolism. While *E. coli*-derived indole mediates the toxic effects of tryptophan, the presence of indole alone is sufficient to exert toxicity, irrespective of bacterial species or metabolic activity.

Sugars do not alleviate indole-induced toxicity in *C. elegans*

We next sought to understand the mechanism by which glucose and other sugars suppress tryptophan toxicity. Transcriptomic profiling (Table S1) revealed that tryptophan exposure leads to the upregulation of numerous UGT genes. Notably, the transcriptional response to tryptophan closely resembles that elicited by indole exposure, as reported previously (Lee *et al*, 2017), suggesting that UGT induction may constitute a host defense mechanism against indole-mediated toxicity. UGT enzymes play a central role in phase II xenobiotic detoxification by conjugating glucose moieties to xenobiotic substrates, thereby increasing their solubility and facilitating excretion. Consistent with this, *C. elegans* has been shown to glycosylate indoles to reduce their toxicity (Stupp *et al*, 2013).

We hypothesized that glucose supplementation may enhance UGT-mediated detoxification by increasing the availability of glucose substrates for conjugation. Under this model, the glycosylation of indoles could be responsible for the observed rescue of tryptophan toxicity when glucose is added. To test this hypothesis, we supplemented indole-containing plates with glucose and assessed egg hatching. Unexpectedly, even 50 mM glucose failed to promote hatching on plates containing 2 mM indole (Figures 6A and S5B), indicating that glucose supplementation does not alleviate indole toxicity. To further evaluate this, we supplemented indole plates with other sugars that were tested for mitigating tryptophan toxicity. However, none of these sugars ameliorated the toxic effects of indole (Figure S5C). These results suggested that sugar-mediated rescue of tryptophan toxicity does not occur via enhanced UGT-mediated glycosylation of indole, and that sugars do not protect *C. elegans* from indole toxicity.

Sugars alleviate tryptophan toxicity by suppressing bacterial indole production

We observed that several sugars alleviate the toxic effects of tryptophan but not those of indole. This suggests that these sugars may act upstream of indole production, potentially preventing tryptophan from being converted into its toxic derivative. We therefore asked whether sugar supplementation affects bacterial indole production. Previous studies have shown that glucose inhibits the activity of tryptophanase, the enzyme responsible for converting tryptophan to indole in bacteria (Botsford & DeMoss, 1971; Li & Young, 2014). Based on these findings, we hypothesized that supplementation of sugars might inhibit tryptophanase activity, thereby reducing indole production even in the presence of excess tryptophan.

To test this, we quantified indole production by bacteria using Kovac's reagent. As expected, *E. coli* cultured in LB medium produced indole under basal conditions, and indole levels were further elevated upon tryptophan supplementation (Figure 6B). Notably, glucose supplementation significantly reduced indole production in cultures exposed to high concentrations of tryptophan (Figure 6B). We extended this analysis to other monosaccharides and disaccharides. Strikingly, only those sugars that rescued tryptophan toxicity also reduced indole production. In contrast, sucrose and maltose, both ineffective at rescuing tryptophan toxicity, did not significantly lower indole levels compared to the tryptophan-only control (Figure 6B). Furthermore, the sugars that alleviated tryptophan toxicity also diminished basal indole production in the absence of exogenous tryptophan (Figure 6C).

Collectively, these findings support a model in which *E. coli* converts tryptophan to indole, which is then taken up by *C. elegans*. At high concentrations, indole is toxic and impairs egg hatching. Various sugars, including multiple monosaccharides and the disaccharide lactose, inhibit indole biosynthesis in *E. coli*, thereby preventing the downstream toxic effects of tryptophan in *C. elegans* (Figure 6D).

Discussion

Our study demonstrates that bacterial metabolism of tryptophan into indole can profoundly impact host physiology and contribute to toxicity. Over 85 bacterial species, including both Gram-positive and Gram-negative, have been reported to express functional tryptophanase and convert tryptophan to indole (Lee & Lee, 2010). Many of these species reside in the human gut, where they efficiently produce indole and its derivatives (Roager & Licht, 2018).

Indeed, indole is the most abundant tryptophan-derived metabolite detected in human feces and mouse cecal contents, accounting for 50-75% of total tryptophan catabolites, with concentrations of 2.6-2.7 mM (Darkoh *et al*, 2015; Dong *et al*, 2020). The indole concentrations could increase further during enhanced tryptophan uptake, as indole concentrations as high as 6.6 mM have been observed in human faeces (Darkoh *et al*, 2015). Therefore, indoles produced by gut microbiota might lead to toxicity under specific circumstances.

Indole and its derivatives exhibit pleiotropic effects on host biology, ranging from beneficial to detrimental, depending on the context (Jaglin *et al*, 2018; Tennoune *et al*, 2022; Yang *et al*, 2023; Perdijk *et al*, 2024; Seymour *et al*, 2024). At moderate concentrations, indole can promote host health. For example, 250 μM indole has been shown to extend healthspan in *C. elegans*, *Drosophila*, and mice via conserved molecular pathways (Sonowal *et al*, 2017, 2023). Indole also supports intestinal homeostasis by enhancing epithelial barrier function, modulating immune responses, and suppressing the colonization of pathogenic bacteria (Bansal *et al*, 2010; Shimada *et al*, 2013; Alexeev *et al*, 2018; Scott *et al*, 2020). Furthermore, indole and its derivatives have been implicated in ameliorating inflammatory bowel disease, hemorrhagic colitis, colorectal cancer, and type 2 diabetes mellitus (Ye *et al*, 2022).

However, at elevated concentrations or in the context of gut dysbiosis, indole and its metabolites can become deleterious. In the liver, indole is converted to indoxyl sulfate, a known uremic toxin linked to systemic toxicity. Indoxyl sulfate has been implicated in the pathogenesis of cardiovascular and chronic kidney diseases (Banoglu *et al*, 2001; Hung *et al*, 2017; Hoibian *et al*, 2018), and is capable of inducing neuroinflammation and neuronal damage (Adesso *et al*, 2017, 2018). Additionally, indole exacerbates portal hypertension in a rat model of liver cirrhosis (Huc *et al*, 2018) and can promote the development of collagen-induced arthritis in mice via microbiota-dependent mechanisms (Seymour *et al*, 2024). In *C. elegans*, high levels of indole reduce lifespan (Lee *et al*, 2017). These observations underscore that the pathological consequences of indole are context-dependent, influenced by its concentration and specific derivatives.

Our findings reveal that several monosaccharides, as well as the disaccharide lactose, inhibit indole production in *E. coli*. Previous studies have shown that glucose and arabinose suppress indole production by inhibiting tryptophanase activity (Botsford & DeMoss, 1971;

Li & Young, 2014). Although catabolite repression via cyclic AMP (cAMP) was initially proposed as the underlying mechanism (Isaacs *et al*, 1994), subsequent studies have shown that tryptophanase regulation also involves cAMP-independent pathways (Li & Young, 2014). Tryptophanase activity is regulated through complex and multilayered networks (Stewart & Yanofsky, 1985; Isaacs *et al*, 1994; Gong & Yanofsky, 2003; Li & Young, 2014), suggesting that indole production may offer evolutionary advantages to bacteria (Boya *et al*, 2021). Indeed, indole serves as a critical signaling molecule in microbial communities and can influence microbial composition (Lee & Lee, 2010; Lee *et al*, 2015). Diets rich in protein and tryptophan may thus promote the proliferation of indole-producing bacteria, potentially leading to gut dysbiosis.

Our results suggest that indole production by gut microbiota can be modulated through dietary interventions. Indeed, dietary components such as fiber, non-starch polysaccharides, and high-fat diets have been shown to reduce gut indole production, shifting tryptophan metabolism toward more beneficial pathways (Knarreborg *et al*, 2002; Krishnan *et al*, 2018; Huang *et al*, 2023; Sinha *et al*, 2024). We identified additional sugars capable of suppressing indole synthesis in *E. coli* and possibly in other bacterial species. Targeted delivery or regulated release of these sugars in the gut may provide a strategy to fine-tune microbial tryptophan metabolism and mitigate the pathological effects associated with excessive indole production.

Materials and methods

Bacterial strains

The following bacterial strains were used in this study: *Escherichia coli* OP50, *E. coli* BW25113, *E. coli* BW25113 Δ*tnaA* mutant, and *Pseudomonas aeruginosa* PA14 Δ*gacA* mutant. Bacterial cultures were grown in Luria-Bertani (LB) broth at 37°C. The *E. coli* BW25113 Δ*tnaA* mutant was from the *E. coli* Keio collection (Baba *et al*, 2006), and was cultured in LB broth supplemented with 25 μg/mL kanamycin. Because *P. aeruginosa* virulence might affect the hatching and development of *C. elegans*, we used the *gacA* mutant, which has drastically reduced virulence (Tan *et al*, 1999). Nematode growth medium (NGM) plates were seeded with the respective bacterial cultures and incubated at room temperature for at least two days prior to use in experiments.

C. elegans strains and growth conditions

C. elegans hermaphrodites were maintained at 20°C on NGM plates seeded with *E. coli* OP50. The Bristol N2 strain was used as the wild-type control. The following strains were used in this study: RG3052 *tdo-2(ve552[LoxP + myo-2p::GFP::unc-54 3' UTR + rps-27p::neoR::unc-54 3' UTR + LoxP])*, RB1190 *amx-2(ok1235)*, and MT15434 *tph-1(mg280)*. Some of the strains were obtained from the Caenorhabditis Genetics Center (University of Minnesota, Minneapolis, MN).

Preparation of NGM plates with different supplements

The following supplements, indicated with their product numbers, were obtained from HiMedia BioSciences: L-tryptophan (#GRM067), D-(+)-glucose (#TC130), D-(-)-fructose (#GRM196), D-(+)-mannose (#RM104), L-(+)-rhamnose (#RM062), D-(+)-galactose (#GRM101), lactose (#GRM017), sucrose (#GRM134), D-(+)-maltose (#GRM3050), and indole (#GRM824). All the supplements were added to the NGM immediately prior to pouring into plates to achieve the desired final concentrations. Indole was dissolved in methanol, and control plates were supplemented with equivalent volumes of methanol for assays involving indole.

C. elegans egg hatching assays

A synchronized egg population was obtained by transferring 15-20 gravid adult hermaphrodites onto NGM plates and allowing them to lay eggs for 1.5-2 hours. After that, the adults were removed, and the number of eggs laid was counted. The plates were then incubated at 20°C, and the number of hatched eggs/L1 larvae was quantified after 24 hours. Representative images of the plates were captured after 96 hours of incubation at 20°C. For each experimental condition, at least three independent biological replicates were performed.

RNA isolation

RNA isolation was performed as described previously (Ravi *et al*, 2023; Rao & Singh, 2025). Briefly, wild-type N2 animals were synchronized by egg laying. Approximately 50 gravid adult hermaphrodites were transferred to 9-cm NGM plates seeded with *E. coli* OP50 and allowed to lay eggs for 4 hours. After removing the adults, the eggs were incubated at 20°C for 72 hours to allow development into adult worms. The adult animals were then collected, washed with M9 buffer, and transferred to *E. coli* OP50-seeded plates containing the following three conditions: control plates without supplements, 2 mM tryptophan, and 2 mM tryptophan plus 50 mM glucose. Following a 6-hour incubation at 20°C, worms were collected, washed with M9 buffer, and snap-frozen in TRIzol reagent (Life Technologies, Carlsbad, CA). Total RNA was extracted using the RNeasy Plus Universal Kit (Qiagen, Netherlands). The RNA samples from three independent biological replicates were isolated for each condition.

RNA sequencing and data analysis

Total RNA was isolated from N2 worms grown under three conditions: control, 2 mM tryptophan, and 2 mM tryptophan plus 50 mM glucose, using three biological replicates per condition, as described above. Library preparation and sequencing were conducted at Unipath Specialty Laboratory Ltd., India. The cDNA libraries were sequenced on the NovaSeq 6000 platform using 150-bp paired-end reads.

The RNA sequencing data were analyzed using the web platform Galaxy (https://usegalaxy.org/), following previously described workflows (Ghosh & Singh, 2024; Rao *et al*, 2024). Briefly, paired-end reads were first trimmed using the Trimmomatic tool. The resulting reads obtained for each sample were mapped to the *C. elegans* reference genome (WS220) using the STAR aligner. Read counts per gene were quantified using the htseq-count tool. Differential gene expression analysis was then performed using DESeq2. Genes exhibiting at least a two-fold change and a *P*-value <0.01 were considered differentially expressed. Gene ontology enrichment analysis was carried out using the DAVID Bioinformatics Resource (https://david.ncifcrf.gov/tools.jsp). Venn diagrams were generated using the BioVenn web tool (https://www.biovenn.nl/), and heatmaps were created using the pheatmap package in R version 4.5.0 (R Statistical Software).

Bacterial killing

Bacterial killing was performed as described previously (Lee *et al*, 2024). Briefly, *E. coli* OP50 was cultured in 50 mL of LB broth at 37°C for 24 hours. The culture was then centrifuged at 3000 × *g* for 30 minutes. The supernatant was discarded, and the bacterial pellet was resuspended in 100 mL of autoclaved water containing 250 µg/mL kanamycin. The suspension was distributed equally into two 250-mL flasks and incubated with shaking at 37°C for an additional 24 hours. To confirm bacterial killing, 1 mL of the culture was aliquoted, washed three times with sterile water, and plated on LB agar. Plates were incubated at 37°C for 24 hours and checked for viable colonies. If no colonies were detected, the bacteria were considered effectively killed and stored at 4°C. Before use, the killed bacterial culture was washed three times with 100 mL of sterile water and concentrated 20-fold before seeding onto NGM plates.

Indole measurement using Kovac's reagent

To prepare samples for indole quantification, various sugars were added to LB broth at a final concentration of 50 mM. Each sugar was added to 10 mL of LB broth in 50 mL tubes, with or without added tryptophan. After that, 20 µL of the same primary culture of *E. coli* OP50 was added into each tube, which were then incubated at 37°C for 12 hours. The optical density at 600 nm (OD_{600}) was measured for all cultures, and the cultures were adjusted to the same OD_{600} prior to indole quantification. As a control, 10 mL of LB broth containing *E. coli* OP50 without added sugar or tryptophan was similarly cultured. Indole standards (0, 0.1, 0.5, 1, 2, 5, and 10 mM) were prepared in LB broth and processed in parallel with the samples to generate a calibration curve.

Indole levels were measured as described previously (Mueller *et al*, 2009), with minor modifications. Briefly, 1 mL of each culture was transferred to a 1.5 mL microcentrifuge tube and centrifuged at 11,300 × *g* for 20 seconds. Then, 250 µL of the supernatant was mixed with 250 µL of 20% (w/v) trichloroacetic acid (Sigma-Aldrich #T6399) and incubated on ice for 15 minutes. The mixture was centrifuged at 13,000 × *g* for 10 minutes to remove precipitated proteins. Subsequently, 450 µL of the resulting supernatant was combined with 500 µL of Kovac's reagent (Sigma-Aldrich #67309) and vortexed. The samples were incubated at room temperature for 2 minutes to allow phase separation. Then, 200 µL of the upper (colored) layer was transferred to 800 µL of ethanol, and absorbance was measured at

540 nm. Indole concentrations were calculated using a standard curve generated on the same day.

Quantification and statistical analysis

The statistical analysis was performed with Prism 8 (GraphPad). All error bars represent the mean ± standard deviation. The unpaired, two-tailed, two-sample *t*-test was employed when needed, and statistical significance was determined when $P < 0.05$. For more than two samples, ordinary one-way ANOVA followed by Dunnett's multiple comparisons test was used. In the figures, asterisks (*) denote statistical significance as follows: $*P < 0.05$; $**P < 0.01$; and $***P < 0.001$, as compared with the appropriate controls. All experiments were performed at least three times.

Acknowledgments

We thank the Caenorhabditis Genetics Center [funded by the NIH Office of Research Infrastructure Programs (P40 OD010440)] for providing the strains used in this study. We thank Ritika Bassi (IISER Mohali) for help with the generation of the heatmap.

Funding

This work was supported by the following grants: STARS grant (File No. MoE-STARS/STARS-2/2023-0116) awarded by the Ministry of Education, India; Har-Gobind Khorana-Innovative Young Biotechnologist Fellowship (File No. HRD-17011/2/2023-HRD-DBT) and Ramalingaswami Re-entry Fellowship (Ref. No. BT/RLF/Re-entry/50/2020) awarded by the Department of Biotechnology, India; Anusandhan National Research Foundation (ANRF) Core Research Grant (Ref. No. CRG/2023/001136) awarded by DST, India; Research Grant (Ref. No. 37/1741/23/EMR-II) awarded by the Council of Scientific & Industrial Research (CSIR), India; and IISER Mohali intramural funds.

Author Contributions

S.G., Subodh, and J.S. conceived and designed the experiments. S.G. and Subodh performed the experiments. S.G. and J.S. analyzed the data and wrote the paper.

Declaration of interests

The authors declare no competing interests.

Data availability

The RNA sequencing data for N2 worms exposed to tryptophan alone and tryptophan plus glucose, along with the control, have been submitted to the public repository, the Sequence Read Archive, with BioProject ID PRJNA1271509. All data generated or analyzed during this study are included in the manuscript and supporting files.

References

Adesso S, Magnus T, Cuzzocrea S, Campolo M, Rissiek B, Paciello O, Autore G, Pinto A & Marzocco S (2017) Indoxyl Sulfate Affects Glial Function Increasing Oxidative Stress and Neuroinflammation in Chronic Kidney Disease: Interaction between Astrocytes and Microglia. *Front Pharmacol* 8: 370

Adesso S, Paterniti I, Cuzzocrea S, Fujioka M, Autore G, Magnus T, Pinto A & Marzocco S (2018) AST-120 Reduces Neuroinflammation Induced by Indoxyl Sulfate in Glial Cells. *J Clin Med* 7: 365

Agus A, Planchais J & Sokol H (2018) Gut Microbiota Regulation of Tryptophan Metabolism in Health and Disease. *Cell Host Microbe* 23: 716–724

Alexeev EE, Lanis JM, Kao DJ, Campbell EL, Kelly CJ, Battista KD, Gerich ME, Jenkins BR, Walk ST, Kominsky DJ, *et al* (2018) Microbiota-Derived Indole Metabolites Promote Human and Murine Intestinal Homeostasis through Regulation of Interleukin-10 Receptor. *Am J Pathol* 188: 1183–1194

Baba T, Ara T, Hasegawa M, Takai Y, Okumura Y, Baba M, Datsenko KA, Tomita M, Wanner BL & Mori H (2006) Construction of Escherichia coli K-12 in-frame, single-gene knockout mutants: the Keio collection. *Mol Syst Biol* 2: 2006.0008

Banoglu E, Jha GG & King RS (2001) Hepatic microsomal metabolism of indole to indoxyl, a precursor of indoxyl sulfate. *Eur J Drug Metab Pharmacokinet* 26: 235–240

Bansal T, Alaniz RC, Wood TK & Jayaraman A (2010) The bacterial signal indole increases epithelial-cell tight-junction resistance and attenuates indicators of inflammation. *Proc Natl Acad Sci U S A* 107: 228–233

500 Bortolotti P, Hennart B, Thieffry C, Jausions G, Faure E, Grandjean T, Thepaut M, Dessein R, Allorge D,
501 Guery BP, *et al* (2016) Tryptophan catabolism in Pseudomonas aeruginosa and potential for
502 inter-kingdom relationship. *BMC Microbiol* 16: 137

503 Botsford JL & DeMoss RD (1971) Catabolite repression of tryptophanase in Escherichia coli. *J*
504 *Bacteriol* 105: 303–312

505 Boya BR, Kumar P, Lee J-H & Lee J (2021) Diversity of the Tryptophanase Gene and Its Evolutionary
506 Implications in Living Organisms. *Microorganisms* 9: 2156

507 Cubero J, Chanclón B, Sánchez S, Rivero M, Rodríguez AB & Barriga C (2009) Improving the quality of
508 infant sleep through the inclusion at supper of cereals enriched with tryptophan, adenosine-
509 5'-phosphate, and uridine-5'-phosphate. *Nutr Neurosci* 12: 272–280

510 Dang H, Castro-Portuguez R, Espejo L, Backer G, Freitas S, Spence E, Meyers J, Shuck K, Gardea EA,
511 Chang LM, *et al* (2023) On the benefits of the tryptophan metabolite 3-hydroxyanthranilic
512 acid in Caenorhabditis elegans and mouse aging. *Nat Commun* 14: 8338

513 Darkoh C, Chappell C, Gonzales C & Okhuysen P (2015) A Rapid and Specific Method for the
514 Detection of Indole in Complex Biological Samples. *Appl Environ Microbiol* 81: 8093–8097

515 Dong F, Hao ,Fuhua, Murray ,Iain A., Smith ,Philip B., Koo ,Imhoi, Tindall ,Alyssa M., Kris-Etherton
516 ,Penny M., Gowda ,Krishne, Amin ,Shantu G., Patterson ,Andrew D., *et al* (2020) Intestinal
517 microbiota-derived tryptophan metabolites are predictive of Ah receptor activity. *Gut*
518 *Microbes* 12: 1788899

519 Edwards C, Canfield J, Copes N, Brito A, Rehan M, Lipps D, Brunquell J, Westerheide SD & Bradshaw
520 PC (2015) Mechanisms of amino acid-mediated lifespan extension in Caenorhabditis elegans.
521 *BMC Genet* 16: 8

522 Fernstrom JD (1983) Role of precursor availability in control of monoamine biosynthesis in brain.
523 *Physiol Rev* 63: 484–546

524 Friedman M (2018) Analysis, Nutrition, and Health Benefits of Tryptophan. *Int J Tryptophan Res IJTR*
525 11: 1178646918802282

526 Gao K, Mu C, Farzi A & Zhu W (2020) Tryptophan Metabolism: A Link Between the Gut Microbiota
527 and Brain. *Adv Nutr* 11: 709–723

528 Ghosh A & Singh J (2024) Translation initiation or elongation inhibition triggers contrasting effects on
529 Caenorhabditis elegans survival during pathogen infection. *mBio* 15: e02485-24

530 Gong F & Yanofsky C (2003) A Transcriptional Pause Synchronizes Translation with Transcription in
531 the Tryptophanase Operon Leader Region. *J Bacteriol* 185: 6472–6476

532 van der Goot AT, Zhu W, Vázquez-Manrique RP, Seinstra RI, Dettmer K, Michels H, Farina F, Krijnen J,
533 Melki R, Buijsman RC, *et al* (2012) Delaying aging and the aging-associated decline in protein
534 homeostasis by inhibition of tryptophan degradation. *Proc Natl Acad Sci* 109: 14912–14917

535 Graboski AL & Redinbo MR (2020) Gut-Derived Protein-Bound Uremic Toxins. *Toxins* 12: 590

536 Haleem DJ (2023) Nutritional importance of tryptophan for improving treatment in depression and
537 diabetes. *Nutr Rev* 81: 133–149

538 He C, Tsuchiyama SK, Nguyen QT, Plyusnina EN, Terrill SR, Sahibzada S, Patel B, Faulkner AR,
539 Shaposhnikov MV, Tian R, *et al* (2014) Enhanced longevity by ibuprofen, conserved in
540 multiple species, occurs in yeast through inhibition of tryptophan import. *PLoS Genet* 10:
541 e1004860

542 Hoibian E, Florens N, Koppe L, Vidal H & Soulage CO (2018) Distal Colon Motor Dysfunction in Mice
543 with Chronic Kidney Disease: Putative Role of Uremic Toxins. *Toxins* 10: 204

544 Hu D, Liu J, Yu W, Li C, Huang L, Mao W & Lu Z (2023) Tryptophan intake, not always the more the
545 better. *Front Nutr* 10

546 Huang Z, Boekhorst J, Fogliano V, Capuano E & Wells JM (2023) Distinct effects of fiber and colon
547 segment on microbiota-derived indoles and short-chain fatty acids. *Food Chem* 398: 133801

548 Huc T, Konop M, Onyszkiewicz M, Podsadni P, Szczepańska A, Turło J & Ufnal M (2018) Colonic indole,
549 gut bacteria metabolite of tryptophan, increases portal blood pressure in rats. *Am J Physiol*
550 *Regul Integr Comp Physiol* 315: R646–R655

551 Hung S, Kuo K, Wu C & Tarng D (2017) Indoxyl Sulfate: A Novel Cardiovascular Risk Factor in Chronic
552 Kidney Disease. *J Am Heart Assoc* 6: e005022

553 Inubushi T, Kamemura N, Oda M, Sakurai J, Nakaya Y, Harada N, Suenaga M, Matsunaga Y, Ishidoh K &
554 Katunuma N (2012) L-tryptophan suppresses rise in blood glucose and preserves insulin
555 secretion in type-2 diabetes mellitus rats. *J Nutr Sci Vitaminol (Tokyo)* 58: 415–422

556 Isaacs H, Chao D, Yanofsky C & Saier MH (1994) Mechanism of catabolite repression of
557 tryptophanase synthesis in Escherichia coli. *Microbiology* 140: 2125–2134

558 Izadi M, Ali TA, Shurrab FM, Aharpour E & Pourkarimi E (2024) Tryptophanyl-tRNA synthetase-1
559 (WARS-1) depletion and high tryptophan concentration lead to genomic instability in
560 Caenorhabditis elegans. *Cell Death Discov* 10: 165

561 Jaglin M, Rhimi M, Philippe C, Pons N, Bruneau A, Goustard B, Daugé V, Maguin E, Naudon L & Rabot
562 S (2018) Indole, a Signaling Molecule Produced by the Gut Microbiota, Negatively Impacts
563 Emotional Behaviors in Rats. *Front Neurosci* 12

564 Ke W, Saba JA, Yao C-H, Hilzendeger MA, Drangowska-Way A, Joshi C, Mony VK, Benjamin SB, Zhang
565 S, Locasale J, *et al* (2020) Dietary serine-microbiota interaction enhances chemotherapeutic
566 toxicity without altering drug conversion. *Nat Commun* 11: 2587

567 Knarreborg A, Beck J, Jensen MT, Laue A, Agergaard N & Jensen BB (2002) Effect of non-starch
568 polysaccharides on production and absorption of indolic compounds in entire male pigs.
569 *Anim Sci* 74: 445–453

570 Krishnan S, Ding Y, Saedi N, Choi M, Sridharan GV, Sherr DH, Yarmush ML, Alaniz RC, Jayaraman A &
571 Lee K (2018) Gut Microbiota-Derived Tryptophan Metabolites Modulate Inflammatory
572 Response in Hepatocytes and Macrophages. *Cell Rep* 23: 1099–1111

573 Le Floc'h N, Otten W & Merlot E (2011) Tryptophan metabolism, from nutrition to potential
574 therapeutic applications. *Amino Acids* 41: 1195–1205

575 Lee J-H, Kim Y-G, Kim M, Kim E, Choi H, Kim Y & Lee J (2017) Indole-associated predator-prey
576 interactions between the nematode Caenorhabditis elegans and bacteria. *Environ Microbiol*
577 19: 1776–1790

578 Lee J-H & Lee J (2010) Indole as an intercellular signal in microbial communities. *FEMS Microbiol Rev*
579 34: 426–444

580 Lee J-H, Wood TK & Lee J (2015) Roles of Indole as an Interspecies and Interkingdom Signaling
581 Molecule. *Trends Microbiol* 23: 707–718

582 Lee Y-U, Fox BW, Guo R, Curtis BJ, Yu J, Kim S, Nanda S, Baumann V, Yilmaz LS, Haynes CM, *et al*
583 (2024) Host-microbe interactions rewire metabolism in a C.elegans model of leucine
584 breakdown deficiency. *Nat Metab* 6: 1584–1600

585 Li G & Young KD (2014) A cAMP-independent carbohydrate-driven mechanism inhibits tnaA
586 expression and TnaA enzyme activity in Escherichia coli. *Microbiol Read Engl* 160: 2079–2088

587 Lindseth G, Helland B & Caspers J (2015) The effects of dietary tryptophan on affective disorders.
588 *Arch Psychiatr Nurs* 29: 102–107

589 Mueller RS, Beyhan S, Saini SG, Yildiz FH & Bartlett DH (2009) Indole acts as an extracellular cue
590 regulating gene expression in Vibrio cholerae. *J Bacteriol* 191: 3504–3516

591 Ooka H, Segall PE & Timiras PS (1988) Histology and survival in age-delayed low-tryptophan-fed rats.
592 *Mech Ageing Dev* 43: 79–98

593 Perdijk O, Butler A, Macowan M, Chatzis R, Bulanda E, Grant RD, Harris NL, Wypych TP & Marsland BJ
594 (2024) Antibiotic-driven dysbiosis in early life disrupts indole-3-propionic acid production
595 and exacerbates allergic airway inflammation in adulthood. *Immunity* 57: 1939-1954.e7

596 Rao R, Aballay A & Singh J (2024) Inhibition of the UFD-1-NPL-4 complex triggers an inflammation-
597 like response in Caenorhabditis elegans. *eLife* 13: RP94310

598 Rao R & Singh J (2025) Innate immune and endoplasmic reticulum unfolded protein response
599 pathways protect Caenorhabditis elegans against chloroquine toxicity. *J Biosci* 50: 15

600 Ravi, Kumar A, Bhattacharyya S & Singh J (2023) Thiol reductive stress activates the hypoxia response
601 pathway. *EMBO J* 42: e114093

602 Roager HM & Licht TR (2018) Microbial tryptophan catabolites in health and disease. *Nat Commun* 9:
603 3294

604 Schwarcz R & Stone TW (2017) The kynurenine pathway and the brain: Challenges, controversies and
605 promises. *Neuropharmacology* 112: 237–247

606 Scott SA, Fu J & Chang PV (2020) Microbial tryptophan metabolites regulate gut barrier function via
607 the aryl hydrocarbon receptor. *Proc Natl Acad Sci U S A* 117: 19376–19387

608 Segall PE & Timiras PS (1976) Patho-physiologic findings after chronic tryptophan deficiency in rats: a
609 model for delayed growth and aging. *Mech Ageing Dev* 5: 109–124

610 Seymour BJ, Trent B, Allen BE, Berlinberg AJ, Tangchittsumran J, Jubair WK, Chriswell ME, Liu S,
611 Ornelas A, Stahly A, *et al* (2024) Microbiota-dependent indole production stimulates the
612 development of collagen-induced arthritis in mice. *J Clin Invest* 134

613 Shimada Y, Kinoshita M, Harada K, Mizutani M, Masahata K, Kayama H & Takeda K (2013) Commensal
614 bacteria-dependent indole production enhances epithelial barrier function in the colon. *PloS*
615 *One* 8: e80604

616 Sinha AK, Laursen MF, Brinck JE, Rybtke ML, Hjørne AP, Procházková N, Pedersen M, Roager HM &
617 Licht TR (2024) Dietary fibre directs microbial tryptophan metabolism via metabolic
618 interactions in the gut microbiota. *Nat Microbiol* 9: 1964–1978

619 Smith T (1897) A MODIFICATION OF THE METHOD FOR DETERMINING THE PRODUCTION OF INDOL
620 BY BACTERIA. *J Exp Med* 2: 543–547

621 Sonowal R, Swimm A, Sahoo A, Luo L, Matsunaga Y, Wu Z, Bhingarde JA, Ejzak EA, Ranawade A,
622 Qadota H, *et al* (2017) Indoles from commensal bacteria extend healthspan. *Proc Natl Acad*
623 *Sci U S A* 114: E7506–E7515

624 Sonowal R, Swimm AI, Cingolani F, Parulekar N, Cleverley TL, Sahoo A, Ranawade A, Chaudhuri D,
625 Mocarski ES, Koehler H, *et al* (2023) A microbiota and dietary metabolite integrates DNA
626 repair and cell death to regulate embryo viability and aneuploidy during aging. *Sci Adv* 9:
627 eade8653

628 Stewart V & Yanofsky C (1985) Evidence for transcription antitermination control of tryptophanase
629 operon expression in Escherichia coli K-12. *J Bacteriol* 164: 731–740

630 Stupp GS, von Reuss SH, Izrayelit Y, Ajredini R, Schroeder FC & Edison AS (2013) Chemical
631 detoxification of small molecules by Caenorhabditis elegans. *ACS Chem Biol* 8: 309–313

632 Tan M-W, Mahajan-Miklos S & Ausubel FM (1999) Killing of Caenorhabditis elegans by Pseudomonas
633 aeruginosa used to model mammalian bacterial pathogenesis. *Proc Natl Acad Sci* 96: 715–
634 720

635 Tennoune N, Andriamihaja M & Blachier F (2022) Production of Indole and Indole-Related
636 Compounds by the Intestinal Microbiota and Consequences for the Host: The Good, the Bad,
637 and the Ugly. *Microorganisms* 10: 930

638 Xue C, Li G, Zheng Q, Gu X, Shi Q, Su Y, Chu Q, Yuan X, Bao Z, Lu J, *et al* (2023) Tryptophan
639 metabolism in health and disease. *Cell Metab* 35: 1304–1326

640 Yang R-Q, Chen Y-H, Wu Q, Tang J, Niu S-Z, Zhao Q, Ma Y-C & Zou C-G (2023) Indole produced during
641 dysbiosis mediates host–microorganism chemical communication. *eLife* 12: e85362

642 Ye X, Li H, Anjum K, Zhong X, Miao S, Zheng G, Liu W & Li L (2022) Dual Role of Indoles Derived From
643 Intestinal Microbiota on Human Health. *Front Immunol* 13: 903526

644 Zhang J, Zhu S, Ma N, Johnston LJ, Wu C & Ma X (2021) Metabolites of microbiota response to
645 tryptophan and intestinal mucosal immunity: A therapeutic target to control intestinal
646 inflammation. *Med Res Rev* 41: 1061–1088

647

Figures

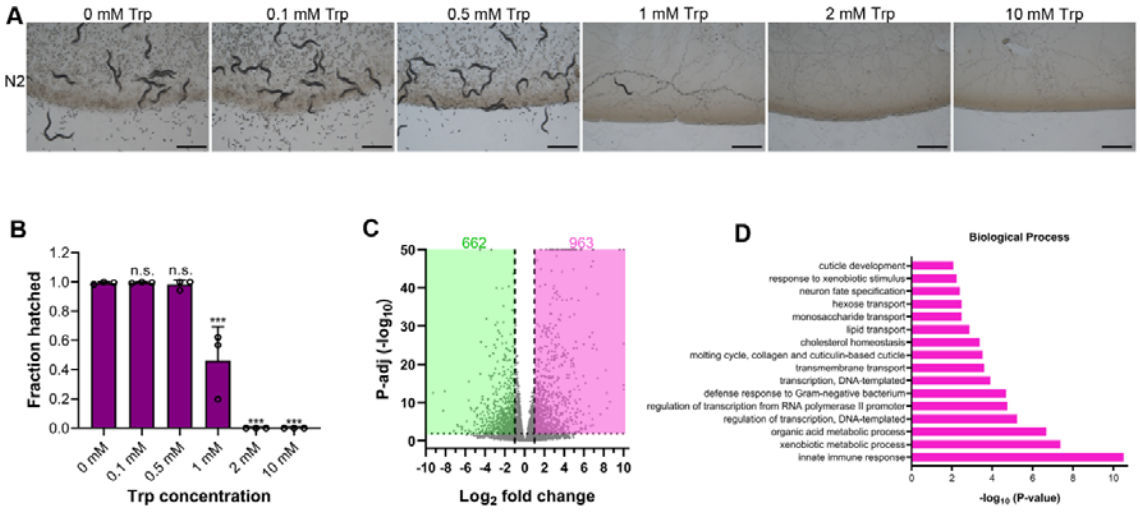

Figure 1. Tryptophan is highly toxic to *C. elegans* and inhibits egg hatching

(A) Representative images of N2 worms on various concentrations of tryptophan (Trp) on *E. coli* OP50 diet after 96 hours of hatching at 20°C. Scale bar = 1 mm.

(B) Quantification of hatched eggs of N2 worms on various concentrations of tryptophan on *E. coli* OP50 after 24 hours of hatching at 20°C. ***$P < 0.001$ and n.s., nonsignificant via ordinary one-way ANOVA followed by Dunnett's multiple comparisons test ($n = 3$ biological replicates).

(C) Volcano plot of upregulated and downregulated genes in N2 worms exposed to 2 mM tryptophan.

(D) Gene ontology enrichment analysis of genes upregulated upon tryptophan exposure for biological processes.

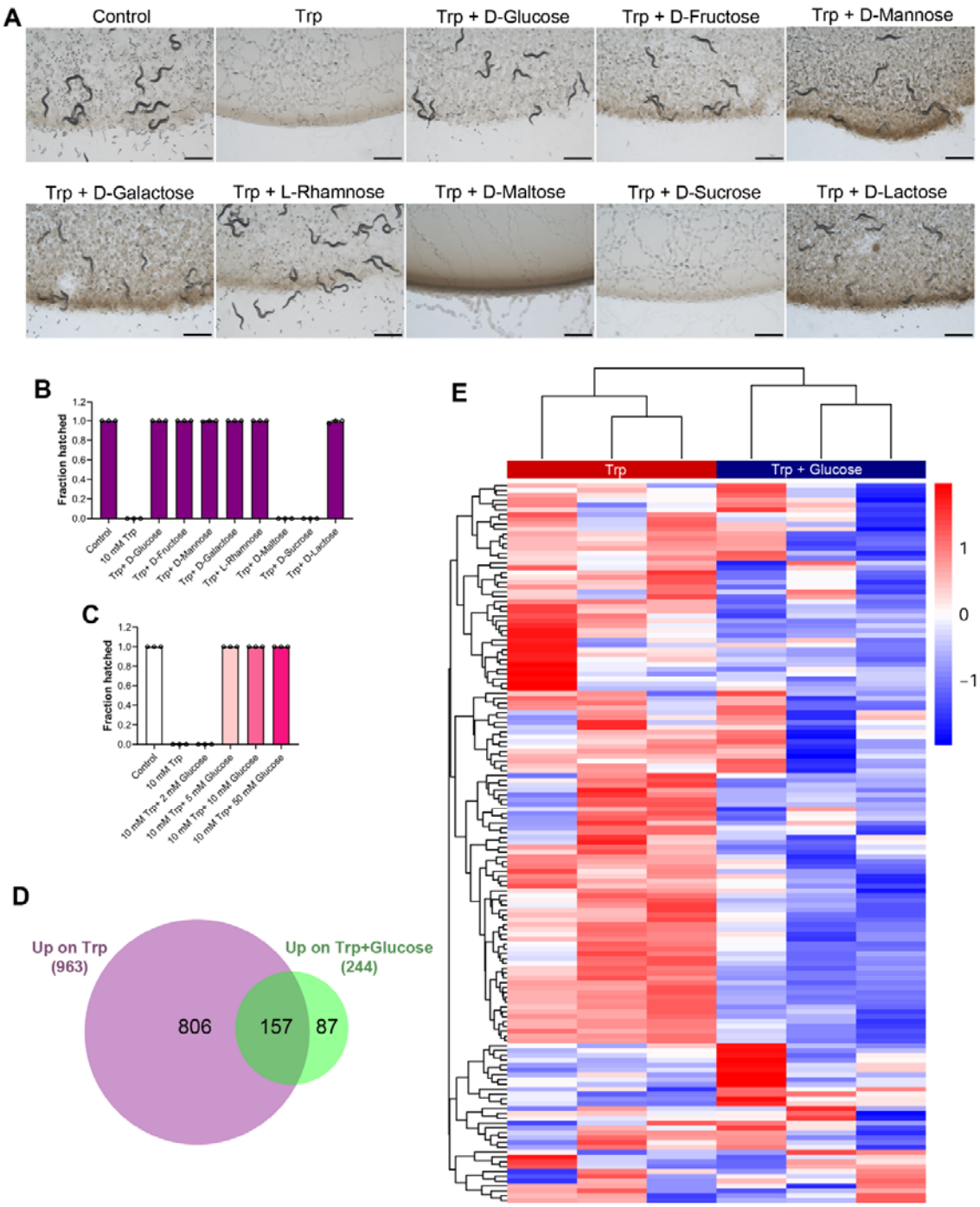

Figure 2. Sugars rescue tryptophan toxicity

(A) Representative images of N2 worms grown on *E. coli* OP50 diet for 96 hours at 20°C containing 0 mM tryptophan (Trp), 10 mM Trp, and 10 mM Trp supplemented with 50 mM of different sugars. Scale bar = 1 mm.

(B) Quantification of hatched eggs of N2 worms grown on *E. coli* OP50 diet for 24 hours at 20°C containing 0 mM Trp, 10 mM Trp, and 10 mM Trp supplemented with 50 mM of different sugars. (n = 3 biological replicates).

(C) Quantification of hatched eggs of N2 worms grown on *E. coli* OP50 diet for 24 hours at 20°C containing 0 mM Trp, 10 mM Trp, and 10 mM Trp supplemented with different concentrations of glucose. (n = 3 biological replicates).

(D) Venn diagram showing the overlap between the genes upregulated upon exposure to 2 mM Trp alone and 2 mM Trp plus 50 mM glucose.

(E) Heat map showing the expression of upregulated genes common between Trp alone and Trp plus glucose.

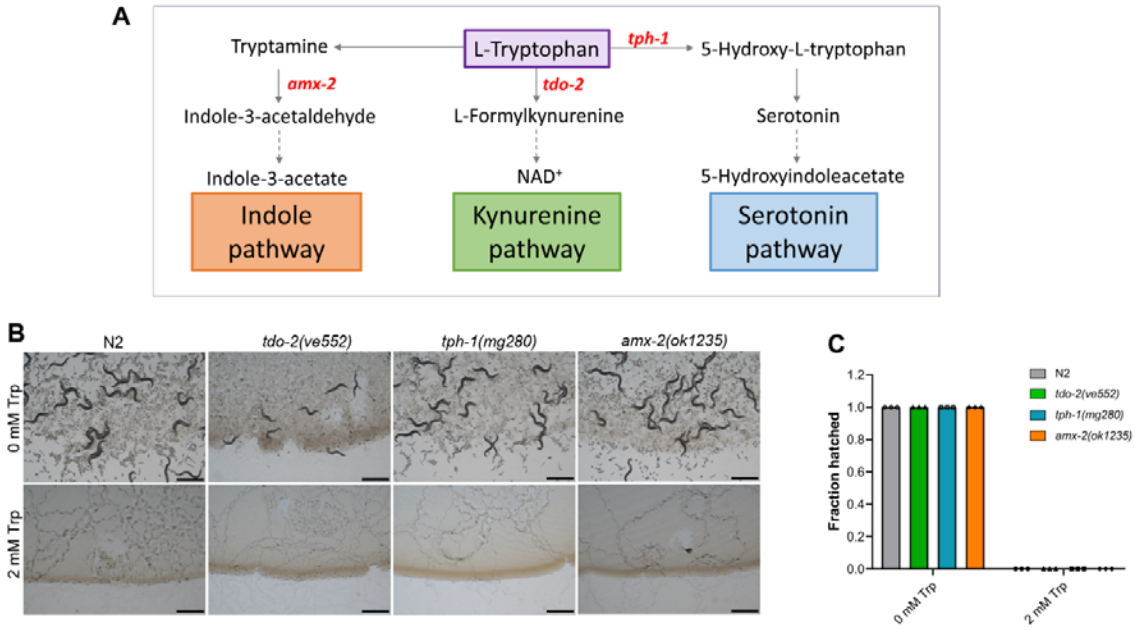

Figure 3. Blocking tryptophan catabolism in *C. elegans* does not alleviate tryptophan toxicity

(A) Simplified representation of tryptophan metabolism pathways. L-tryptophan is metabolized in *C. elegans* via three main pathways: the kynurenine, indole, and serotonin pathways.

(B) Representative images of N2, *tdo-2(ve552)*, *tph-1(mg280)*, and *amx-2(ok1235)* worms after 96 hours of hatching at 20°C on *E. coli* OP50 diet containing 0 mM and 2 mM tryptophan (Trp). Scale bar = 1 mm.

(C) Quantification of hatched eggs of N2, *tdo-2(ve552)*, *tph-1(mg280)*, and *amx-2(ok1235)* worms after 24 hours of hatching at 20°C on *E. coli* OP50 diet containing 0 mM and 2 mM Trp. (n = 3 biological replicates).

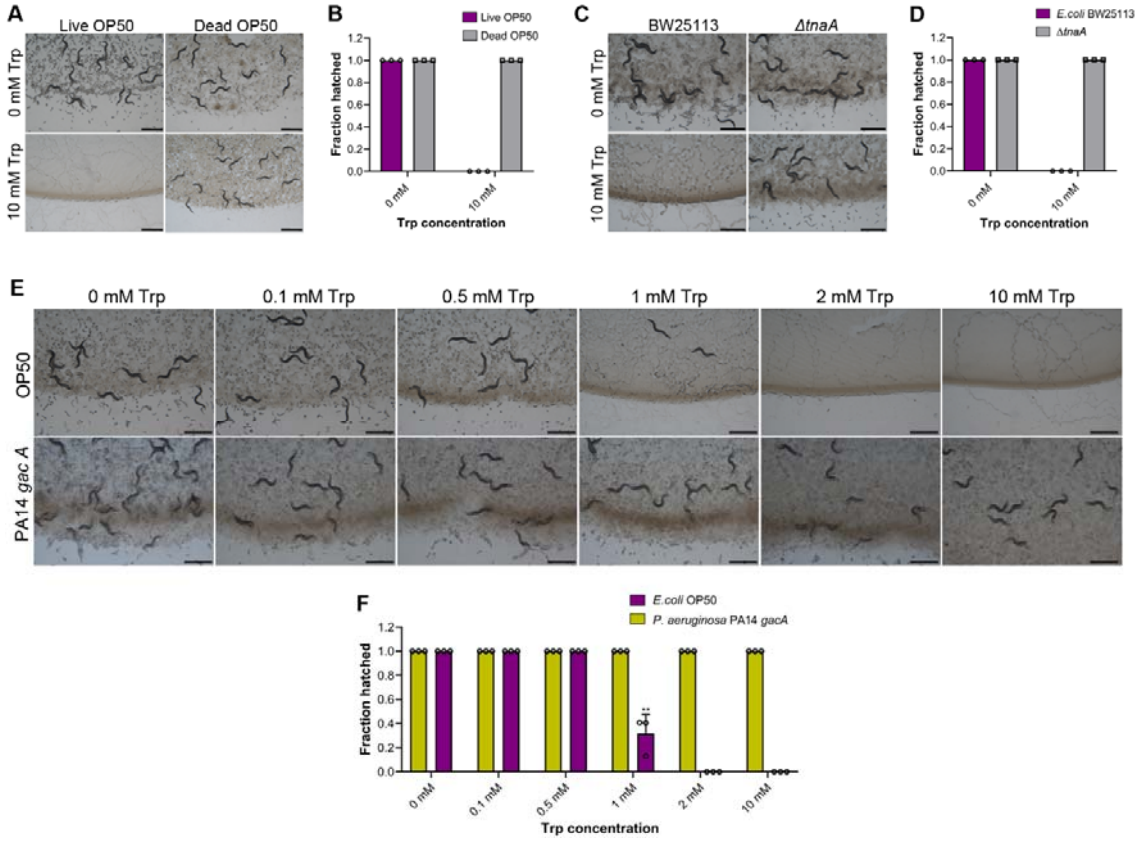

Figure 4. Bacterial metabolism of tryptophan is essential for its toxicity in *C. elegans*

(A) Representative images of N2 worms after 96 hours of hatching at 20°C on live and dead *E. coli* OP50 diet containing 0 mM and 10 mM tryptophan (Trp). Scale bar = 1 mm.

(B) Quantification of hatched eggs of N2 worms after 24 hours of hatching at 20°C on live and dead *E. coli* OP50 diet containing 0 mM and 10 mM Trp. (n = 3 biological replicates).

(C) Representative images of N2 worms after 96 hours of hatching at 20°C on wild-type *E. coli* BW25113 and Δ*tnaA* mutant diet containing 0 mM and 10 mM Trp. Scale bar = 1 mm.

(D) Quantification of hatched eggs of N2 worms after 24 hours of hatching at 20°C on wild-type *E. coli* BW25113 and Δ*tnaA* mutant diet containing 0 mM and 10 mM Trp. (n = 3 biological replicates).

(E) Representative images of N2 worms after 96 hours of hatching at 20°C on various concentrations of Trp on *E. coli* OP50 and *P. aeruginosa* PA14 diets. Scale bar = 1 mm.

(F) Quantification of hatched eggs of N2 worms after 24 hours of hatching at 20°C on various concentrations of Trp on *E. coli* OP50 and *P. aeruginosa* PA14 diets. ***$P < 0.001$ via the t-test (n = 3 biological replicates).

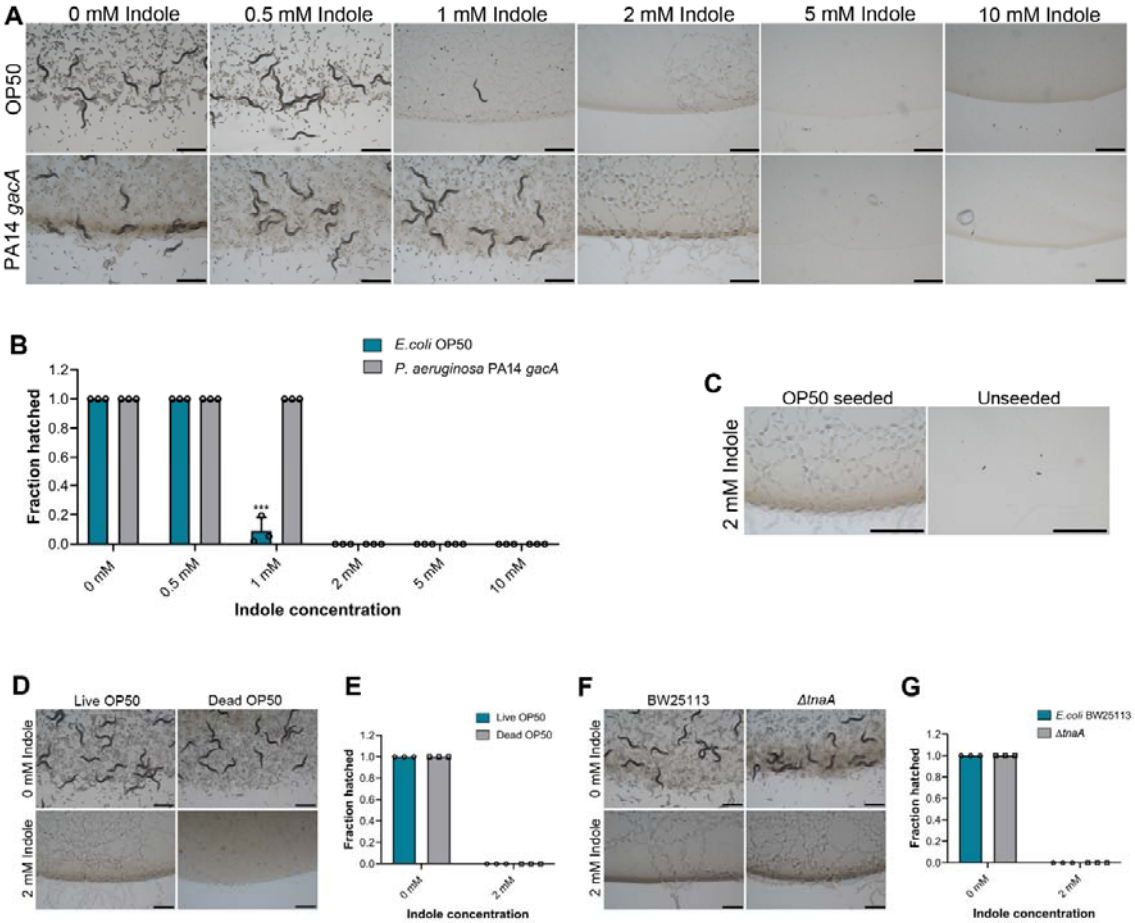

Figure 5. Indole causes toxicity in *C. elegans*

(A) Representative images of N2 worms after 96 hours of hatching at 20°C on various concentrations of indole on *E. coli* OP50 and *P. aeruginosa* PA14 diets. Scale bar = 1 mm.

(B) Quantification of hatched eggs of N2 worms after 24 hours of hatching at 20°C on various concentrations of indole on *E. coli* OP50 and *P. aeruginosa* PA14 diets. ***$P < 0.001$ via the *t*-test ($n = 3$ biological replicates).

(C) Representative images of N2 worms after 24 hours of hatching at 20°C on unseeded and *E. coli* OP50-seeded plates supplemented with 2 mM indole. Scale bar = 1 mm.

(D) Representative images of N2 worms after 96 hours of hatching at 20°C on live and dead *E. coli* OP50 diet containing 0 mM and 2 mM indole. Scale bar = 1 mm.

(E) Quantification of hatched eggs of N2 worms after 24 hours of hatching at 20°C on live and dead *E. coli* OP50 diet containing 0 mM and 2 mM indole. ($n = 3$ biological replicates).

(F) Representative images of N2 worms after 96 hours of hatching at 20°C on wild-type *E. coli* BW25113 and Δ*tnaA* mutant diet containing 0 mM and 2 mM indole. Scale bar = 1 mm.

(G) Quantification of hatched eggs of N2 worms after 24 hours of hatching at 20°C on wild-type *E. coli* BW25113 and Δ*tnaA* mutant diet containing 0 mM and 2 mM indole. ($n = 3$ biological replicates).

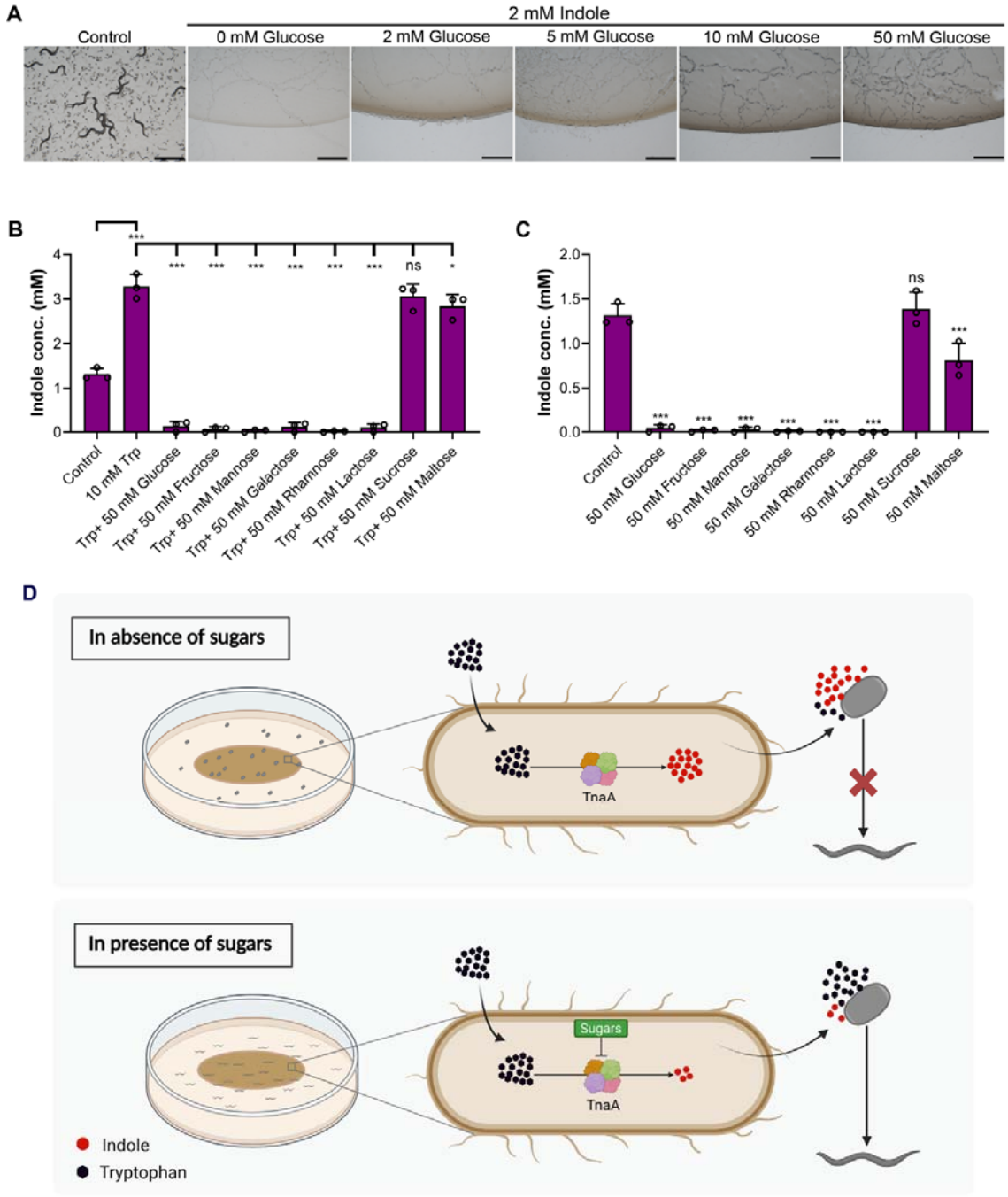

Figure 6. Sugars alleviate tryptophan toxicity by suppressing bacterial indole production

(A) Representative images of N2 worms grown on *E. coli* OP50 diet for 96 hours at 20°C containing 0 mM indole, 2 mM indole, and 2 mM indole supplemented with increasing concentration of glucose. Scale bar = 1 mm.

(B) Quantification of indole produced by *E. coli* OP50 cultured without any supplement, with 10 mM tryptophan (Trp), and with 10 mM Trp plus 50 mM of various sugars. *$P < 0.05$,

***$P < 0.001$, and n.s., nonsignificant via ordinary one-way ANOVA followed by Dunnett's multiple comparisons test ($n = 3$ biological replicates).

(C) Quantification of indole produced by *E. coli* OP50 cultured without any supplement and with 50 mM of various sugars. ***$P < 0.001$ and n.s., nonsignificant via ordinary one-way ANOVA followed by Dunnett's multiple comparisons test ($n = 3$ biological replicates). The control data in (B) and (C) are the same.

(D) Model showing that the bacterial metabolism of tryptophan causes toxicity in *C elegans*. *E. coli* takes up tryptophan and catabolizes it to indole via tryptophanase (TnaA). Indole can freely diffuse through lipid membranes and prevents hatching of worm eggs at high concentrations. The addition of sugars decreases indole production from tryptophan by inhibiting TnaA in *E. coli*, resulting in the hatching and development of *C. elegans* in the presence of excessive tryptophan.

Supplementary Figures

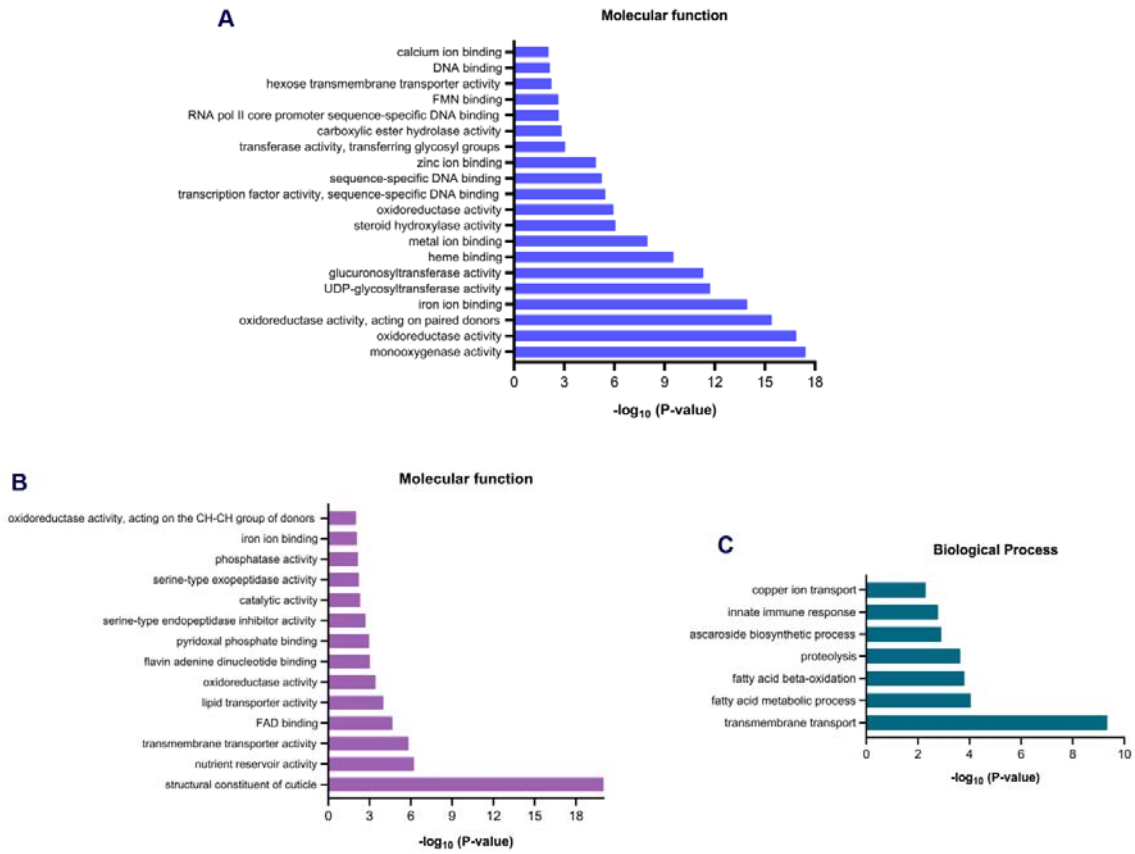

Figure S1. Gene ontology analysis for genes differentially regulated upon tryptophan exposure

(A) Gene ontology enrichment analysis of genes upregulated upon tryptophan exposure for molecular function.

(B)-(C) Gene ontology enrichment analysis of genes downregulated upon tryptophan exposure for molecular function (B) and (C) biological processes.

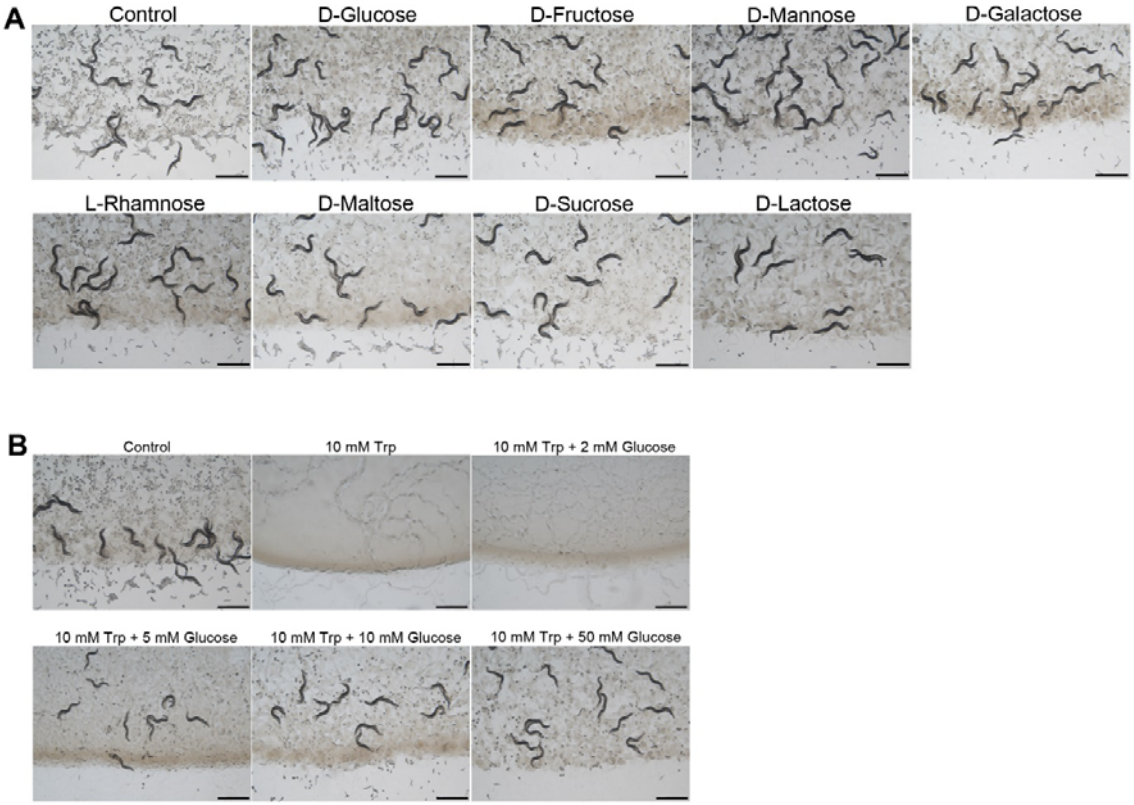

Figure S2. Sugars rescue tryptophan toxicity

(A) Representative images of N2 worms grown on *E. coli* OP50 diet for 96 hours at 20°C supplemented with 50 mM of different sugars. Scale bar = 1 mm.

(B) Representative images of N2 worms grown on *E. coli* OP50 diet for 96 hours at 20°C containing 0 mM Trp, 10 mM Trp, and 10 mM Trp supplemented with different concentrations of glucose. Scale bar = 1 mm.

Figure S3. Sugars rescue tryptophan toxicity

Venn diagram showing the overlap between the genes downregulated upon exposure to 2 mM Trp alone and 2 mM Trp plus 50 mM glucose.

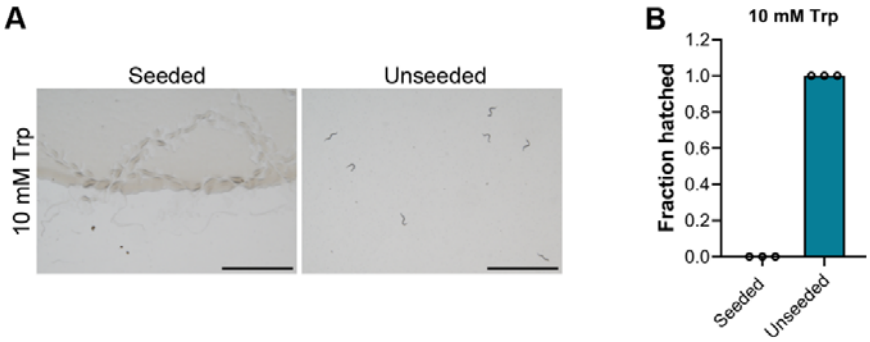

Figure S4. Bacterial metabolism of tryptophan is essential for its toxicity in *C. elegans*

(A) Representative images of N2 worms after 24 hours of hatching at 20°C on unseeded and *E. coli* OP50-seeded plates supplemented with 10 mM tryptophan (Trp). Scale bar = 1 mm.

(B) Quantification of hatched eggs of N2 worms after 24 hours of hatching at 20°C on unseeded and *E. coli* OP50-seeded plates supplemented with 10 mM Trp. (n = 3 biological replicates).

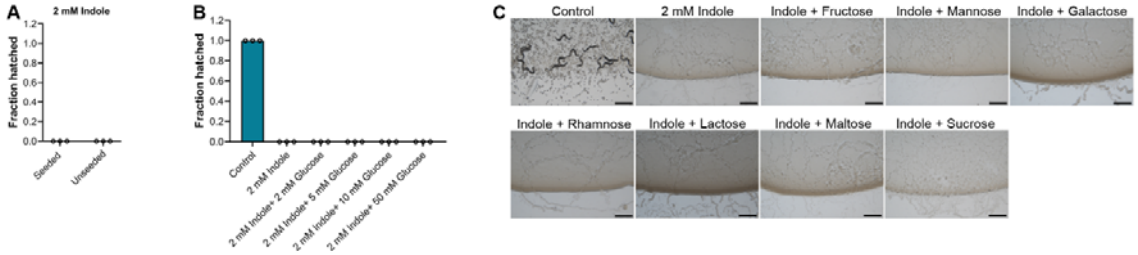

Figure S5. Sugars do not alleviate indole-induced toxicity in *C. elegans*

(A) Quantification of hatched eggs of N2 worms after 24 hours of hatching at 20°C on unseeded and *E. coli* OP50-seeded plates supplemented with 2 mM indole. (n = 3 biological replicates).

(B) Quantification of hatched eggs of N2 worms grown on *E. coli* OP50 diet for 24 hours at 20°C containing 0 mM indole, 2 mM indole, and 2 mM indole supplemented with different concentrations of glucose. (n = 3 biological replicates).

(C) Representative images of N2 worms grown on *E. coli* OP50 diet for 96 hours at 20°C containing 0 mM indole, 2 mM indole, and 2 mM Indole supplemented with 50 mM of different sugars. Scale bar = 1 mm.

Supplementary Table

Table S1. Differentially-regulated genes in adult N2 worms exposed to 2 mM tryptophan for 6 hours. A separate Excel file is provided.

Table S2. Differentially-regulated genes in adult N2 worms exposed to 2 mM tryptophan plus 50 mM glucose for 6 hours. A separate Excel file is provided.

Table S3. Comparison of genes upregulated in N2 worms upon exposure to tryptophan alone and tryptophan plus glucose. A separate Excel file is provided.

Table S4. Comparison of genes downregulated in N2 worms upon exposure to tryptophan alone and tryptophan plus glucose. A separate Excel file is provided.